

Journal of Stress Analysis

Vol. 8, No. 1, 2023-24, 69-81



ORIGINAL RESEARCH PAPER

Analysis of Influences of Parameters on Hydrostatic Compressive Stress in Cyclic Extrusion Compression Angular Pressing for CP-Ti

Behzad Pasoodeh^a, Vali Alimirzaloo^{a,*}, Mehrdad Shahbaz^b, Kaveh Hajizadeh^c, Javad Alizadeh Kaklar^a

- ^a Department of Mechanical Engineering, Faculty of Engineering, Urmia University, Urmia, Iran.
- ^b Department of Material Engineering, Faculty of Engineering, Urmia University, Urmia, Iran.
- ^c Department of Mining and Metallurgical Engineering, Urmia University of Technology, Urmia, Iran.

Article info

Article history:
Received 20 January 2023
Received in revised form
08 May 2023
Accepted 22 September 2023

Keywords: CECAP process OP observation Hydrostatic compressive stress Response surface method Finite element analysis CP-Ti

Abstract

Cyclic extrusion compression angular pressing (CECAP) is a new severe plastic deformation method used to improve mechanical and metallurgical properties of metals. In this process, hydrostatic compressive stress has a considerable effect on the quality of the fabricated sample, where, as it rises, the probability of the appearance of the crack initiation on the sample is reduced. In this research, the effects of the process parameters of CECAP on magnitude and distribution of the hydrostatic compressive stress were investigated using finite element analysis (FEA) and response surface method (RSM). Temperature (T), input extrusion diameter (D), exit extrusion angle (α) , frictional coefficient (μ) , and longitudinal distance of input extrusion to extrusion compression angular pressing (ECAP) region (L) were selected as input parameters, and hydrostatic compressive stress (σ) was considered as response variable. Analysis of Variance (ANOVA) was extracted to evaluate the accuracy of the developed mathematical model and determine the significant factors. Results revealed that parameters of temperature and exit extrusion angle influence the hydrostatic compressive stress (σ) considerably. Also, the effect of interaction between the parameters is significant. The optical microstructure on the CECAPed section revealed that, for point C (center of section), the grain size is larger, reaching 3 μ m, while for point A (near to outer surface), the grain size reaches 1.5 μ m, showing that as it becomes near to the section, the grain size tends to be smaller. In order to verify the accuracy of the study, the hardness distribution behavior was compared by the strain distribution behavior obtained from finite element method (FEM). Moreover, the hydrostatic compressive stress of the current CECAP process was compared with other investigations and a significant improvement was observed. All experimental tests and the results of other investigations showed a good agreement with FEM results.

E-mail address: v.alimirzaloo@urmia.ac.ir doi 10.22084/JRSTAN.2023.27392.1233

ISSN: 2588-2597



^{*}Corresponding author: V. Alimirzaloo (Assistant Professor)

Nomenclature

T	Temperature	D	Input extrusion diameter
α	Exit extrusion angle	$\parallel \mu$	Frictional coefficient
σ	Hydrostatic compressive stress	$\ \sigma_i \ $	Hydrostatic compressive stress
$\mid L$	Longitudinal distance of input extrusion	N	Number of selected points on the cross
	to ECAP region		section
σ_{ace}	Average hydrostatic compressive stress		

1. Introduction

Due to the suitable characteristics of titanium and its alloys, e.g., Ti-6Al-4V such as corrosion behavior, mechanical properties, and biocompatibility, they have received great attention among investigators in the field of fabricating biomedical equipment [1,2]. Recently, researchers have focused on the production of bulk nanostructured and ultrafine-grained materials by severe plastic deformation (SPD). Many investigators have focused on the modification, improvement, and development of new SPD methods, because of excellent advantages such as improved mechanical characteristics and grain refinement [3, 4]. Although, titanium allovs (here Ti-6Al-4V) have better strength compared to commercially pure titanium (CP-Ti), the release of toxic metal ion by alloying elements and biological incompatibility has restricted application [5, 6]. Thus, CP-Ti can be a perfect choice for medical purposes, provided that its strength is improved by grain refinement. Cyclic extrusion compression angular pressing (CECAP) is one of those techniques producing nanostructured materials [7]. CECAP is the best choice to refine CP-Ti grain size $<1\mu m$ for medical goals, enhancing its strength and obtaining an ultrafine-grained titanium (UFG-Ti) structure [8].

Cyclic Extrusion Compression (CEC) is one of the well-known SPD techniques producing high plastic strain. In the current procedure, an initially cylindrical sample goes through two similar cylindrical channels with the same diameter linked via a reduced cross section neck (extrusion). In each pass of the CEC, first of all, it applies an extrusion followed by compression in the second channel helped by backpressure to retain its initial diameter. However, in order to retain the initial diameter, the backpressure needs to be applied for the reverse compression in the second channel of CEC, which is known as the main problem with the current method. To solve this drawback, a new technique namely cyclic expansion-extrusion (CEE) was proposed to eliminate the backpressure from the CEC process [9, 10]. In this technique, as the material meets the outlet channel, its movement is temporarily obstructed causing the material to expand under pressure. However, the investigations showed that nonuniform material flow in the longitudinal section of the sample over the extrusion and expansion is the main problem with this method [11]. Extrusion compression angular pressing (ECAP) is another widelyknown SPD method satisfying comprehensively SPD demands. Moreover, wide variety of materials such as Zn-Al alloys, Al-Mg alloys, Pb-Sn alloys, AZ91 alloy, AZ31 alloy, and Titanium alloys have been examined by this technique [12]. In spite of owning excellent properties of the ECAPed samples, studies revealed that strain inhomogeneity on the sample sections can be considered as main disadvantages of the current procedure [13,14]. To solve the mentioned disadvantages of CEC and ECAP processes, CECAP was proposed combining the advantages of CEC and ECAP methods by M. Ensafi et al. [15]. In this process, in the first step, the initial cylindrical sample goes through a compression extrusion (input) before meeting ECAP region. Then, as the sample reaches ECAP area, due to the applied pressure, the sample starts to fill the gap between CEC and ECAP region resulting in the sample restoring its initial diameter. Due to the combination of the CEC and ECAP advantages simultaneously on the CECAP, the accumulative applied strain is equal to the sum of strains in CEC and ECAP processes. Although it owns higher degrees of strains, it suffers from lower hydrostatic compression stresses on CECAPed samples, which is known as the method's drawback. Thus, in order to solve that problem, S. Ahmadi et al. [7] proposed a novel CECAP process improving the hydrostatic compression stress and uniformity on CECAPed samples. In their method, an extrusion region was added to the outlet channel. In this technique, the lack of hydrostatic compressive stress and strain non-uniformity was compensated by the second extrusion plays. Mg alloy was examined to verify the effectiveness of the proposed procedure by calculation of the grain refinement and stresses. They achieved the contour distribution of the mean stresses applied to the sample section for two conditions, with (CECAP+Extrusion) and without (CECAP) the secondary extrude, respectively. They reported that as the forehead of the sample reaches in the secondary extruded zone, the reduction of diameter applies a backpressure and rises the hydrostatic compression stress. Having done a comparative study for two cases, it was revealed that in the presence of the secondary extrusion, more uniform and larger compression stresses are appeared. The mean stresses calculated by FEM for the novel CECAP process represents a considerable increase of compressive stresses in both paths compared to the CECAP process. In another survey, they also [16] studied the microstructure and mechanical properties of AM60 magnesium alloy by a newly proposed CECAP method. Results indicated that the proposed and CECAP-processed conditions created higher hardness values increasing constantly, where this increase in hardness reported 196% and 175% for the proposed CECAP and conventional CECAP procedure after tolerating four passes compared to the unprocessed samples, respectively.

In this paper, the influences of the input parameters including temperature (T), input extrusion diameter (D), exit extrusion angle (α), friction coefficient (μ) , and longitude distance of input extrusion to ECAP region (L) on the response parameters of hydrostatic compressive stress (σ) were analyzed. In the CECAP process, hydrostatic compressive stress has a significant influence on the quality of the fabricated sample, where as it increases, the probability of crack initiation on the sample is diminished. Furthermore, due to the lack of sufficient investigations on analysis of CP-Ti (with excellent medical applications) processed by CE-CAP with the mentioned input parameters, it was decided to study this material. To meet this target, FEM and RSM methods were implemented to examine the CECAP process. Moreover, ANOVA was performed to specify the significant parameters.

2. Principles of CECAP

As mentioned previously, the CECAP process is a recently developed SPD method with two interchangeable extrusion inserts mounted on the prior and after of the ECAP deformation region as illustrated in Fig. 1. This method includes two cylindrical channels shown by D (here 15mm), and an ECAP deformation zone consisting of corner angle ψ (here 20°), and channel angle φ (here 90°). Once operation starts, the initial cylindrical sample pass through the input extrusion zone with a 2-mm-reduction. Afterward, due to the pressure applied by the end of vertical cylindrical channel (ECAP region), the sample tends to expand and restores its initial diameter (15mm). Then, the sample tolerates the strain applied by the ECAP area and enjoys more strains. And finally, the sample meets the exit extrusion region at the end of the horizontal channel. This step not only applies a diameter reduction by 1mm to the sample, it also plays an important role in creating the hydrostatic compressive stress affecting damage and quality of the CECAPed sample.

3. Materials and Experimental Method for CECAP

In the current paper, a commercial CP-Ti grade 2 in the form of cold extruded rod was utilized whose chemical composition is shown in Table 1.

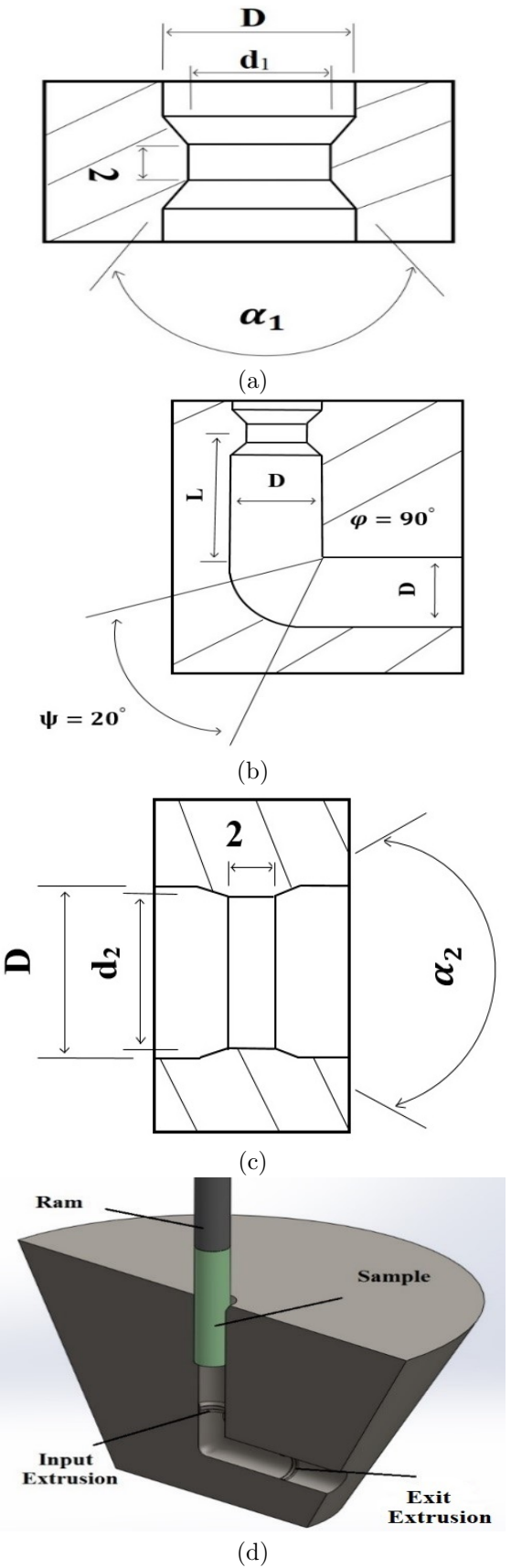


Fig. 1. Input Extrusion zone b) ECAP region c) Exit Extrusion zone d) CECAP model.

In addition, the as-received optical microscopic (OM) microstructure of the used CP-Ti with an average grain size of 15 μ m is shown in Fig 2. For the purpose of OM observation, the selected zones were polished with 0.05 μm colloidal silica and etched in a solution containing $2\%HF+6\%HNO_3+92\%H_2O$. In the current experimental tests, a ram speed of 0.25mm/sec was used for various conditions. Moreover, the CE-CAP die and hydraulic press shown in Fig. 3 were applied to experimental testes. This CECAP die includes the diameters of 13mm, 15mm, and 14mm for the input extrusion zone, the ECAP zone, and exit extrusion zone, respectively. The temperature of $250^{\circ}C$ was used to perform experimental testes. A ceramic heater was used to rise the sample temperature for performance, as shown in Fig. 3c. To investigate the accuracy of the proposed FEM model, the hardness of the experimentally fabricated specimen was measured and compared to FEM results. Vickers microhardness measurements were carried out by applying 10s dwell time and 30g load with a loading rate of 4g/s. The tests were performed on the cross section perpendicular to the sample's moving axis. Moreover, to enhance the accuracy of the performed testes, the indentation was repeated five times at each location on the sections, and the average microhardness values were reported.

 Table 1

 Chemical composition of used CP-Ti in the current work.

Element	О	N	Fe	\mathbf{Pd}	Mg	\mathbf{Cr}
Percentage volume (%)	0.19	0.03	0.14	0.19	0.12	0.2

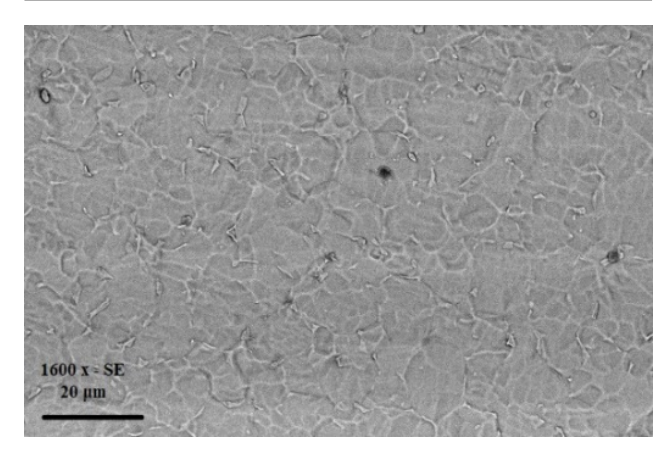
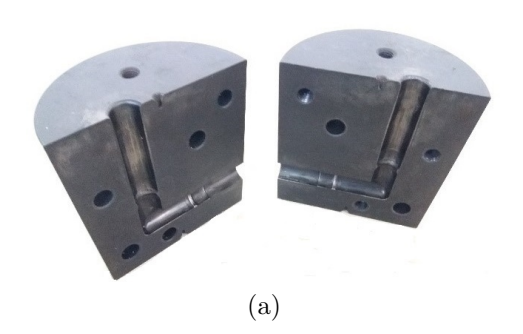
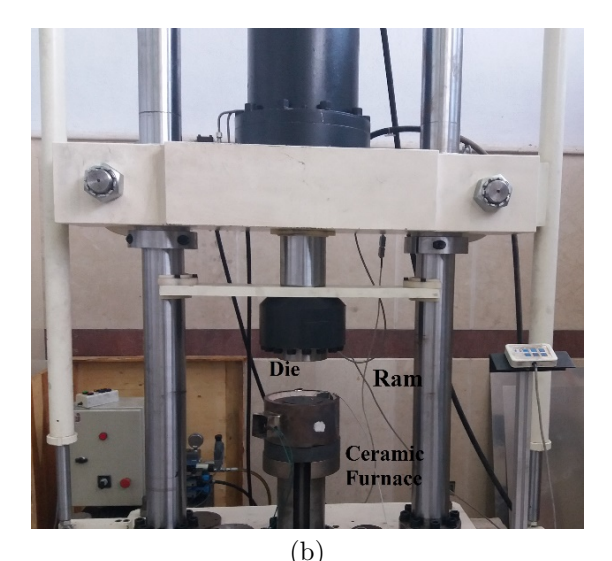


Fig. 2. As-received CP-Ti for OM observation.





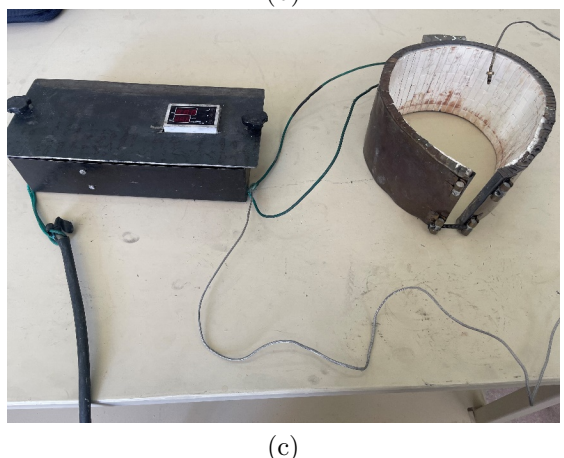


Fig. 3. a) Schematic representation of the current designed CECAP die set, and b) Press applied for experimental process c) Ceramic heater for experimental testl.

4. Finite Element Method

In order to simulate RSM experiment set, commercial Deform-3D V11 software with 3D model was employed. The sample was designed to be plastic owning cylindrical shape with a height of 70mm and a diameter of 15mm. Moreover, the CECAP die and ram were assumed to be rigid bodies in the FEM analysis. A tetrahedral mesh with a minimum mesh size of 0.8mm was selected in this study. The mesh convergence criterion was applied to determine precise mesh numbers and then, a tetrahedral element with a total number of 56000 was selected. The automatic remeshing option was activated to accommodate large deformation over simulation. All analyses were performed at a ram speed of 0.25mm/s. In order to determine the stress-strain relation and consequently achieving simulation constants at selected temperatures, the software library was used for CP-Ti grade 2 and its properties are shown in Table 2 and Fig. 4.

Table 2
Properties of used material.

Poisson's ratio	Young's modulus
	$250^{\circ}C = 103$ GPa
0.3	$300^{\circ}C = 101$ GPa
	$350^{\circ}C = 100$ GPa

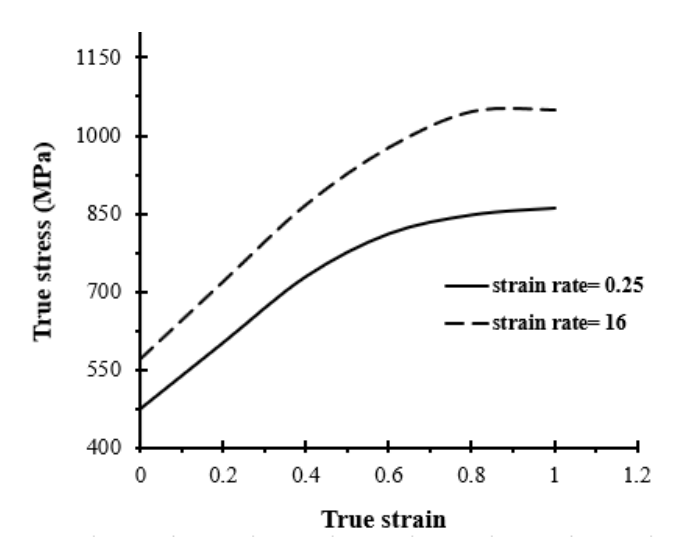


Fig. 4. True stress-strain diagram for the current CP-Ti used in this study for two different strain rates.

5. Response Surface Methodology (RSM)

Die geometrical parameters of CECAP such as input and exit extrusion angle, input extrusion diameter, and the longitude distance of input extrusion to the ECAP region, and process parameters such as temperature, strain rate, and frictional condition have significant effects on the quality and improvement of the response parameters of the CECAPed samples. Thus, extracting the relation between input and response parameters play a considerable role in the successful performance of the CECAP process. In this study, Design Expert V11 software was used to extract the RSM's central composite design (CCD) set of experiments with four input variables in four levels (Table 3). The levels for each of factors in the RSM study, stated in Table 3, were considered from Refs. [7,15,16] and the authors'

knowledge. Temperature (T), input extrusion diameter (D), exit extrusion angle (α), friction coefficient (μ) , and longitudinal distance of input extrusion to ECAP region (L) were considered as input variables and hydrostatic compressive stress (σ) was selected as response variable. A total of 30 experimental testes (24) separate experiments with six repetitions of the central point) were obtained as shown in Table 4. ANOVA was performed to verify the effectiveness of the proposed mathematical model. It was also used to determine the significant factors by calculating a p-value lower than 0.05. The higher values and uniform distribution of the hydrostatic compressive stresses can significantly influence the strain distribution where as it rises, the strain homogeneously distributes throughout the obtained specimen [16] Quantitative relations namely standard deviation (SD) was used to represent non-homogeneity of stress written by Eqs. (1) and (2) [17], respectively, as follows:

$$S.D = \sqrt{\frac{\sum_{i=1}^{n} (\sigma_i - \sigma_{ave})^2}{n}}$$
 (1)

$$\sigma_{ave} = \frac{\sum_{i=1}^{N} (\sigma_i)}{N} \tag{2}$$

Where, σ_i and σ_{ave} represent the effective hydrostatic compressive stress at the i_{th} point and the average hydrostatic compressive stress, respectively. N is the number of selected points on the cross section.

6. Results and Discussion

In order to examine the accuracy and effectiveness of the proposed mathematical RSM-based model, and also to determine significant factors, ANOVA was implemented as illustrated in Table 5. In this analysis, F value represents whether the variance between the means of two populations is significantly different or not, where as the F value increases, the relative variance among the group means improves. The p-value presented by ANOVA is an important criterion determining the significant factors and their percentage contribution in response, where if p-value for an individual factor is calculated less than 0.05, it means that the factor can be considered as a significant factor.

Table 3
Process Parameters and their levels involved in the analysis.

Levels variables	Index	Level 1	Level 2	Level 3
Temperature $(T, {}^{\circ}C)$	A	250	300	350
Input extrusion diameter (D, mm)	В	11	12	13
Exit extrusion angle $(\alpha, degree)$	\mathbf{C}	50	60	70
Friction coefficient (μ)	D	0.2	0.3	0.4
Longitude distance of input extrusion to ECAP region (L, mm)	\mathbf{E}	12	15	18

Table 4
Experimental design matrix and response values in CECAP for CP-Ti

OF-	11.					
Experiment	Temperature (T)	Input extrusion diameter (D)	Exit extrusion $angle(\alpha)$	Frictional coefficient (μ)	Longitude distance of inputextrusion to ECAP region (L)	Standard deviation (hydrostatic compressive stress) (S.D)
1	250	11	50°	0.2	18	26
2	350	11	50°	0.2	12	19.5
3	250	13	50°	0.2	12	16.75
4	350	13	50°	0.2	18	41.6
5	250	11	70°	0.2	12	68.5
6	350	11	70°	0.2	18	52.9
7	250	13	70°	0.2	18	41.8
8	350	13	70°	0.2	12	21.9
9	250	11	50°	0.4	12	58.1
10	350	11	50°	0.4	18	18
11	250	13	50°	0.4	18	47.8
12	350	13	50°	0.4	12	23.5
13	250	11	70°	0.4	18	48.6
14	350	11	70°	0.4	12	19.7
15	250	13	70°	0.4	12	32.6
16	350	13	70°	0.4	18	35.5
17	250	12	60°	0.3	15	28.4
18	350	12	60°	0.3	15	42.7
19	300	11	60°	0.3	15	28.5
20	300	13	60°	0.3	15	35.7
21	300	12	50°	0.3	15	44.6
22	300	12	70°	0.3	15	61.6
23	300	12	60°	0.2	15	32.7
24	300	12	60°	0.4	15	45.1
25	300	12	60°	0.3	12	43
26	300	12	60°	0.3	18	35.5
27	300	12	60°	0.3	15	32.9
28	300	12	60°	0.3	15	32.9
29	300	12	60°	0.3	15	32.9
30	300	12	60°	0.3	15	32.9
31	300	12	60°	0.3	15	32.9
32	300	12	60°	0.3	15	32.9

Ultimately, the results achieved from the p-value and F-value in the ANOVA table denote that among CECAP input factors, A and C, and the interaction of AB, AD, AE, BE, and CD influence the SD of hydrostatic compressive stress (σ) considerably. Moreover, the results revealed that input extrusion diameter, frictional coefficient, and longitude distance of input extrusion to the ECAP region are not significant factors in the current analysis. In the ANOVE table, DOF, Seq-SS, Adj-SS, and Adj-MS represent the degrees of

freedom of parameters, the sequential sums of squares, the adjusted sum of squares, and the adjusted mean squares, respectively. Finally, the mathematical formulation between input variables and standard deviation for hydrostatic compressive stress are presented according to Eq. 3, as follows:

Standars Deviation (S.D) = 37.1084 - 6.5194A - 1.0305B + 5.4416C - 0.0916D + 2.7027E + 6.1718AB - 0.2968AC - 5.1343AD + 4.9781AE - 4.7906BC + 3.0468BD + 5.4843BE -6.0468CD + 1.8406CE - 1.8968DE (3)

Table 5 ANOVA of results for the CECAP process to identify significant factors in hydrostat compressive stress (σ) .

Source	DOF	Seq-SS	Adj-SS	Adj-MS	F-value	P-value
Model	20	5119.36	5119.36	255.96	3.2	0.026
A: (T)	1	765.06	765.06	765.05	9.55	0.01
B:(D)	1	19.12	19.12	19.11	0.24	0.635
C: (α)	1	533.01	533.01	533.01	6.66	0.026
D: (μ)	1	0.15	0.15	0.15	00	0.966
E: (L)	1	131.49	131.49	131.49	1.64	0.226
AB	1	609.47	609.47	609.47	7.61	0.019
AC	1	1.41	1.41	1.41	0.02	0.897
AD	1	421.79	421.79	421.79	5.27	0.042
AE	1	396.51	396.51	396.51	4.95	0.048
$_{\mathrm{BC}}$	1	367.2	367.2	367.2	4.59	0.055
BD	1	148.54	148.54	148.54	1.85	0.2
BE	1	481.25	481.25	481.25	6.01	0.032
CD	1	585.04	585.04	585.04	7.31	0.021
CE	1	54.21	54.21	54.21	0.68	0.428
DE	1	57.57	57.57	57.57	0.72	0.415

Fig. 5 illustrate surface plots to examine the influences of temperature (T), input extrusion diameter (D), exit extrusion angle (α), frictional coefficient (μ) , and longitudinal distance of input extrusion to the ECAP region (L) on the standard deviation of hydrostatic compressive stress. Comparison of the curvature of surface plots in Fig. 5a shows that there is an interaction between temperature and input extrusion diameter which is in a good agreement with ANOVA results. As shown in Fig. 5a, increasing the temperature decreases the stress. However, the effect of increasing input extrusion diameter on stress depends on temperature. This is because of the simultaneous synergetic effects of the large plastic flow (due to the input extrusion diameter) and ease of deformation (due to the higher temperature) [15,16,18]. Figs. 5b and c state the interaction influences of the frictional condition versus exit extrusion angle, and input extrusion diameter and longitudinal distance of input extrusion to ECAP region, showing a suitable agreement with results obtained from ANOVA outcomes.

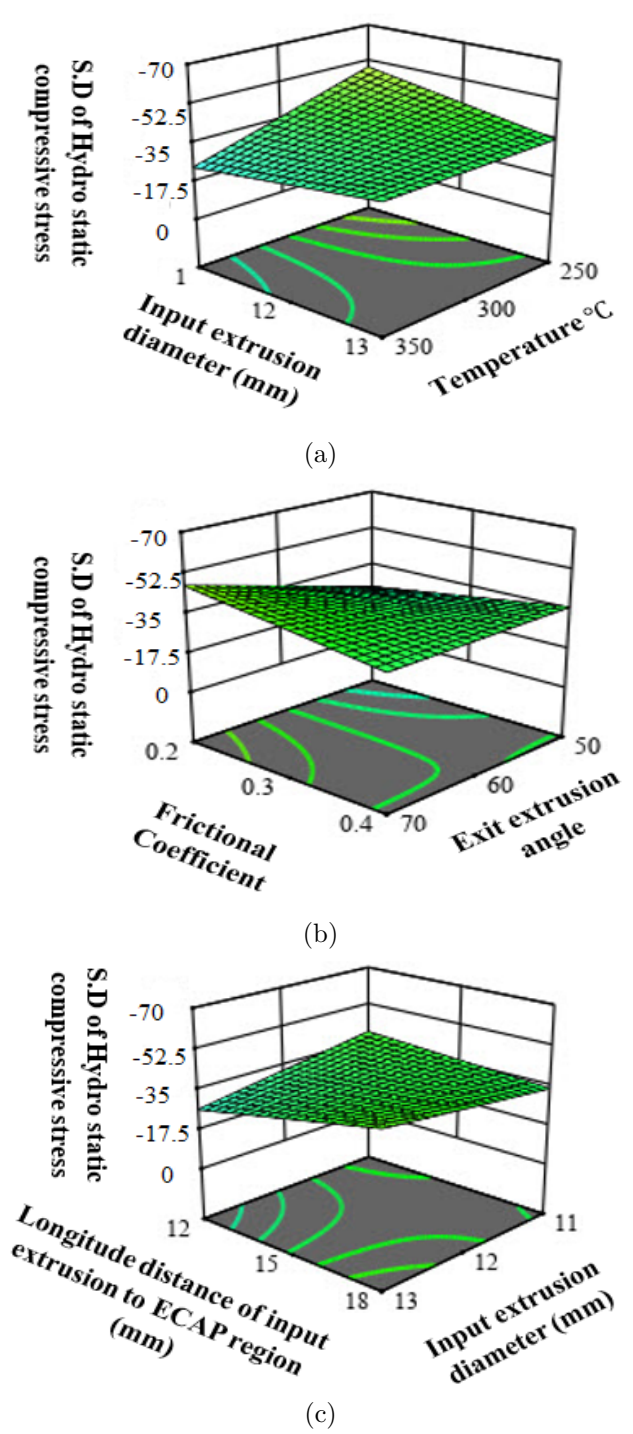
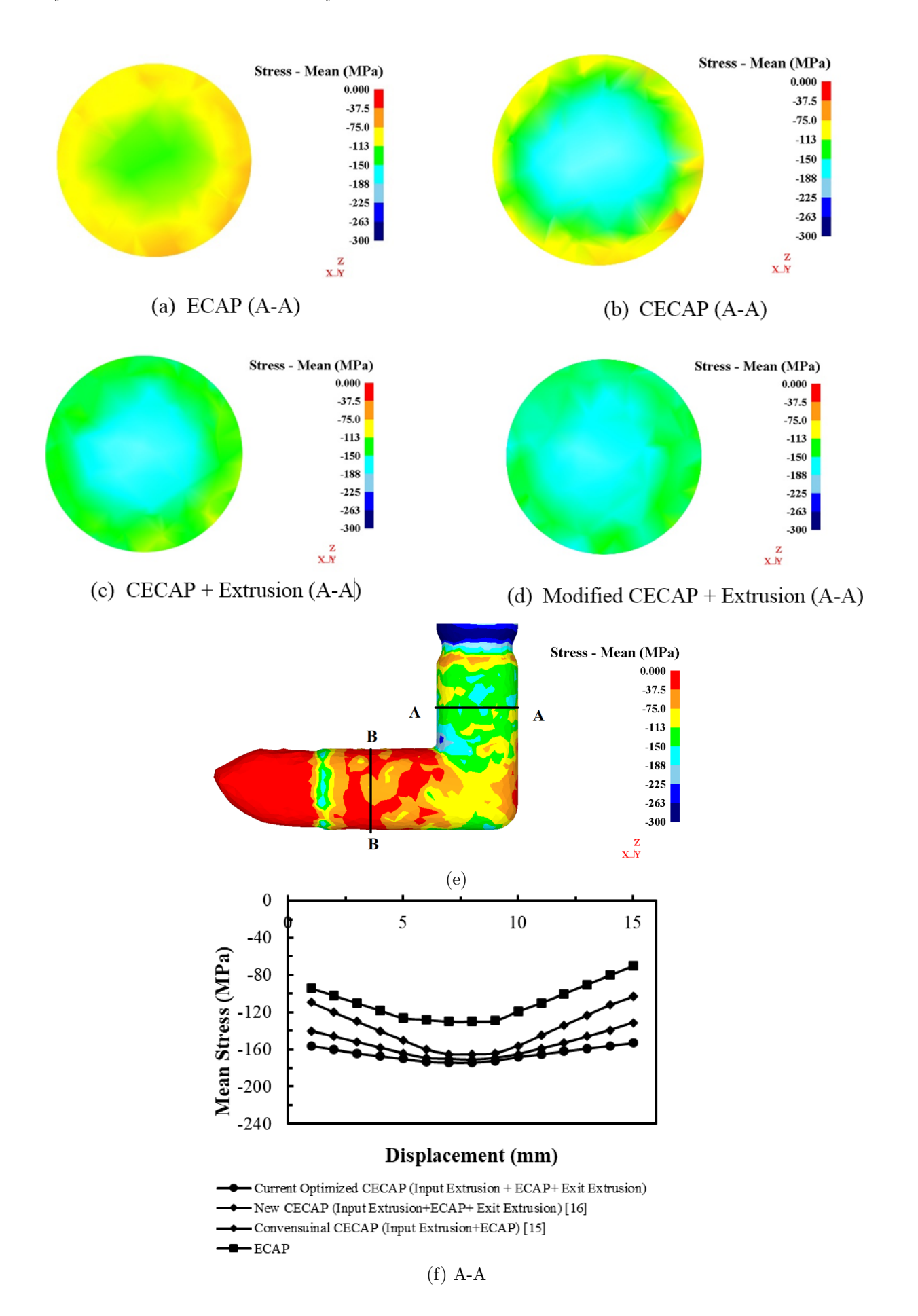


Fig. 5. 3D surface plots of the effects of input factors on SD of the hydrostatic compressive stress (σ) in current CECAP process.

Fig. 6 illustrates the contour distribution of the hydrostatic compressive stress for four different processes on the cross section perpendicular to the moving axis in the zones after first extrusion and before exit extrusion zones, illustrated by A and B in Fig. 6e. Figs. 6a, b, c, and d show ECAP, the conventional CECAP (Input extrusion+ECAP) [15], new CECAP (Input extrusion+ECAP+Exit extrusion) [16], and the current

optimized CECAP, respectively. The hydrostatic compressive stress values enjoy the maximum values in the new CECAP (developed by [7] used in this study) and the current optimized CECAP methods, because in these two processes, once the top of the sample meets in the secondary extruded zone, the diameter reduction in the exit extrusion provides a backpressure and increases the hydrostatic compression stress. Moreover, as the angle of the extrusion increases, the resistance towards the sample movement is created and, subsequently, the hydrostatic compressive stress is improved. Beside this, the presence of the exit extrusion region causes the ECAP area to be completely filled by the sample, which is one of the brilliant advantages of the new CECAP. In conventional CECAP and ECAP processes, due to the lack of an exit extrusion region, the lower backpressure is applied to the sample and the probability of crack initiation is increased. Fig. 6f reveals the diagram of the hydrostatic compressive stress (or mean stress) values for the mentioned four methods in the area after first extrusion (path A). As it is seen, the current method achieves the higher values where it meets its maximum values at central parts of the sample. Although the current method has higher values compared to other approaches, it almost equates to the new CECAP at central parts of the sample. However, in Fig. 6g (path B), the comparison of the current optimized CECAP and the new CECAP shows an approximately constant difference in all of the domain.

The exit extrusion angle acts as backpressure to the process affecting the increase of the hydrostatic compression stress on the whole length of the specimen. This increase causes the section of the achieved specimen to be fabricated uniformly [7] and also reduce the probability of crack initiation and propagation on the specimen [16]. Fig. 7 shows the influence of the exit extrusion angle, frictional coefficient, and ram speed on the hydrostatic compressive stress for the cross sections perpendicular to the moving axis before the ECAP zone. The results revealed that the increase of the ram speed causes the average of the stresses to be reduced slightly regardless of the frictional condition. However, this rise seems to be intensive in higher angles. This behavior is because of the multi-dimension effects of the higher angles and higher ram speeds, meaning that as the ram speeds rise, the influence of the higher exit extrusion angles is more considerable than lower angles. At lower speeds, due to the low velocity and movement of dislocation while passing grain boundaries and another barrier, the plastic flow comes across with difficulties and causes the stresses to increase. In addition, at higher speeds, due to the lack of complete filling of the area between input extrusion and ECAP zones, and consequently, reducing hydrostatic compressive stress, the values of the hydrostatic compressive stress start to drop for higher ram speeds as illustrated in Fig. 8.



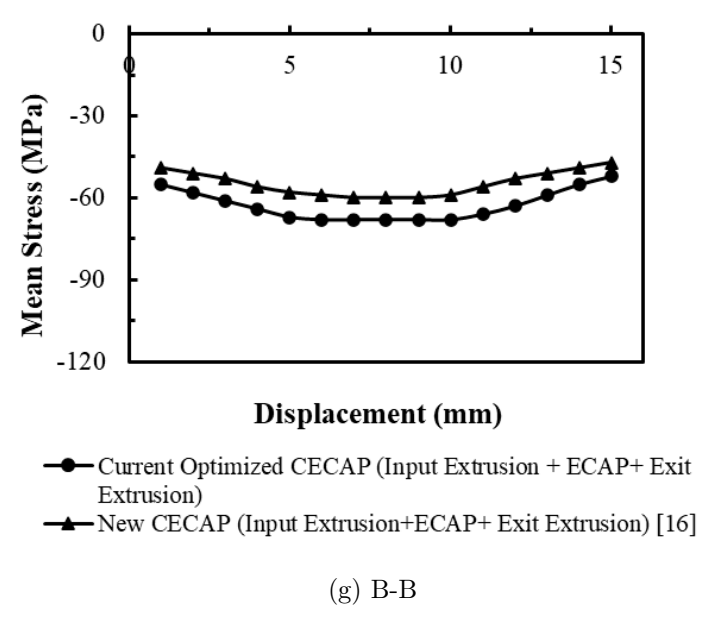
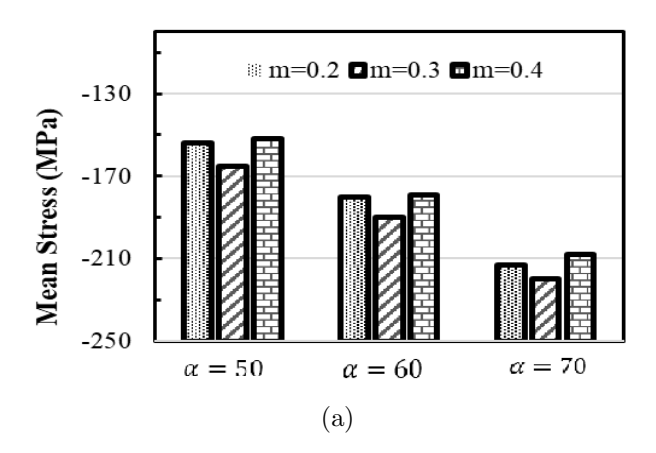


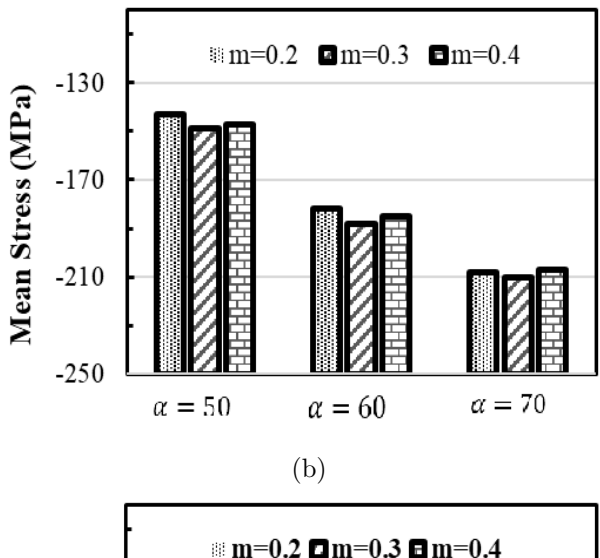
Fig. 6. Distribution of the hydrostatic compressive stress for four different processes: a) ECAP, b) CECAP (Input extrusion+ECAP) [15], c) New CECAP (Input extrusion+ECAP+Exit extrusion) [16], d) Current optimized CECAP (Input extrusion+ECAP+Exit extrusion), e) Contour of simulated sample, f) Comparative study of mean stress on path A, and g) Path B.

Additional achievement from Fig. 7 disclosed that for lower ram speeds, the influence of the frictional condition on hydrostatic compressive stress for various angles shows an optimal point, meaning that the stress starts to fall after a certain value of the frictional condition. However, this condition is not carried out for higher speeds, where the stress tends to go up at higher speeds as the frictional condition rises.

Fig. 9 states the effects of the exit extrusion angle on hydrostatic compressive stress for different longitude distance of input extrusion to the ECAP region shown by L. The outcomes show that as the exit extrusion angles rises, the hydrostatic compressive stress increases slightly in all domain of the horizontal axis (shown by exit extrusion angle). A glance at the provided graph depicts a steady upward trend up to an angle of 63° for L=13mm, but after that value, the slopes start to be smooth on the rest of the angles reaching -62 MPa at an angle of 75°. Further analyses disclosed that as the longitude distance of input extrusion to the ECAP region (L) rises, the mean stress drops almost linearly. This behavior is due to the formation of a larger space before the ECAP zone, needing more backpressure applied by the ECAP area to fill that area and improve the hydrostatic compressive stress.

The experimental CECAPed specimen of CP-Ti in the current CECAP process was performed to verify the validity of the proposed FEM model, as shown on Fig. 10. Thus, the load-stroke diagram for both experimental and FEM specimens were achieved. In addition, the hardness was measured for fabricated specimens. The measurements were performed on the cross sections perpendicular to the moving axis before and after of the ECAP zone in the CECAP process, as shown on Fig. 10b. Fig. 8 compares the distribution behavior for the hardness obtained from the experiments and the strain obtained from FEM. In Fig. 11b for the current CECAP, the hardness in section A at the points near to the center and outer surfaces of the sample reach 20 and 24 HRC, respectively, where the maximum variation for hardness was calculated at about 16% throughout the cross section. The hardness distribution in section B shows a steady fine downward trend dropping from the upper part of the sample to down at the centers of the sample, which is in a good agreement with the distribution model of the strain. Fig. 11a demonstrates the effective strain distribution on sections A and B. As it is seen, the distribution behavior is the same as hardness distribution, where the strain decreases as it goes near to the centers of the sample.





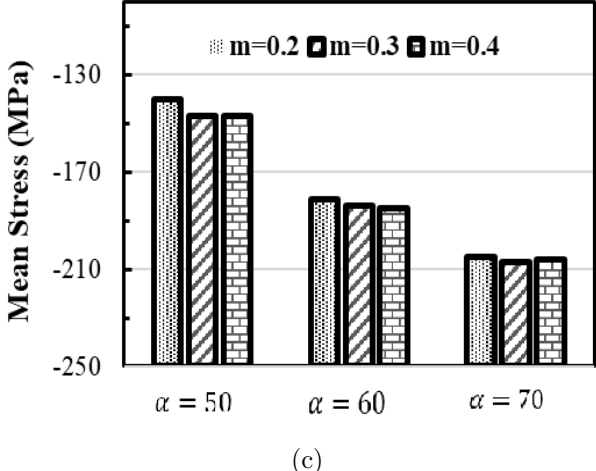


Fig. 7. Influence of the exit extrusion angle, frictional coefficient and ram speed on hydrostatic compressive stress on the cross section perpendicular to moving axis before ECAP zone (Initial sample diameter 15mm, input extrusion diameter of 13mm, longitude distance of input extrusion to ECAP region

L=15mm and temperature of T=350°C all conditions).

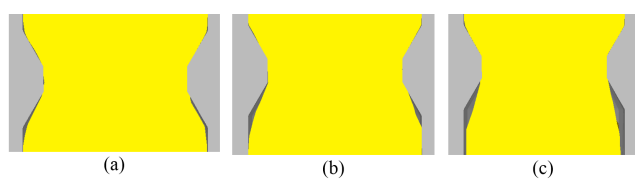


Fig. 8. Influence of ram speed on filling area and consequently hydrostatic compressive stress on the area between input extrusion and ECAP and zones a) Ram speed = 0.15mm/sec b) Ram speed = 0.25mm/sec c) Ram speed = 0.35mm/sec.

Fig. 12 shows a typical OM microstructure of CP-Ti after the CECAP process extracted from the transverse section, depicting grain refinement. As expected, there is a significant refinement in grain size compared to the as-received microstructure (Fig. 2). A glance at the graph provided in Fig. 12 revealed that the majority of deformed grains were enlarged and that a very

lamellar fine structure is appeared. The average deformed grain size for the current CECAP was reduced to 100 nm, which is considerably smaller than that for the as-received material. A more comparative investigation of strain inhomogeneity from the longitudinal section of the processed sample in Fig. 12 disclosed that the microstructure of the current CECAP is significantly composed of grains, which seems to be less elongated on C than on point A. Thus, it can be concluded that although there is a small quantitative difference in the strain inhomogeneity in the OM observation among points, the elongation of deformed grains for the current CECAP on point A is a little more. Moreover, for point C, the grain size is larger reaching 3 μ m, while the grain size reaches 1.5 μ m for point A.

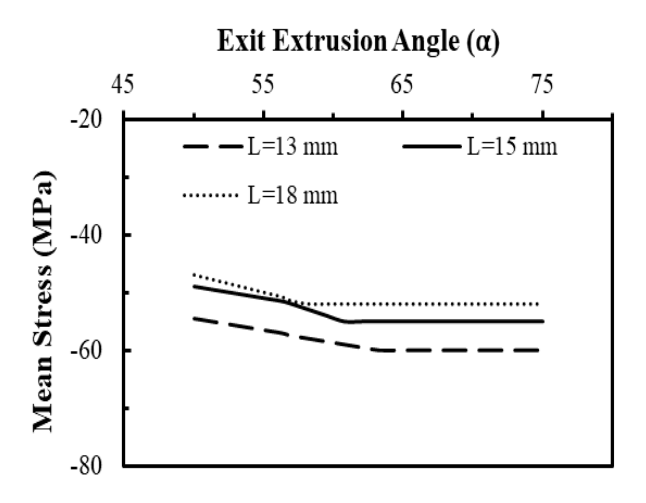
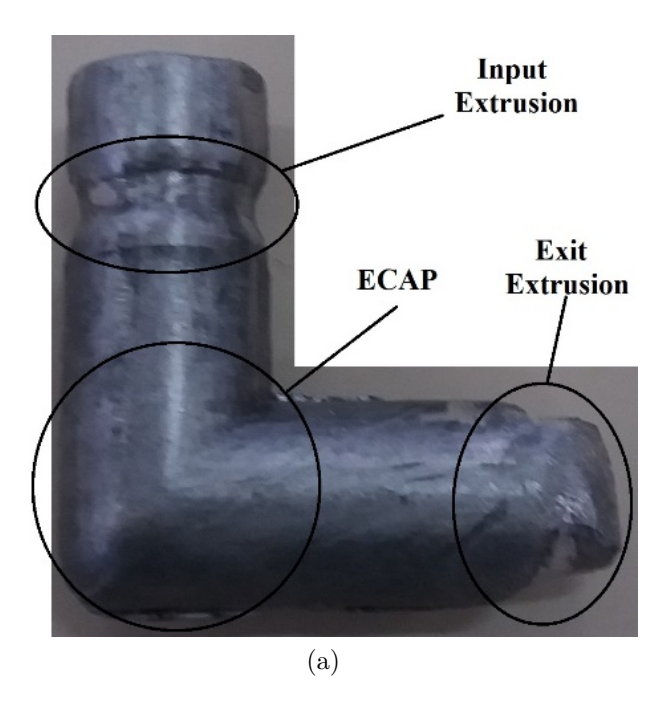


Fig. 9. The effects of the exit extrusion angle on the hydrostatic compression stress for the current CECAP after ECAP zone for various L.



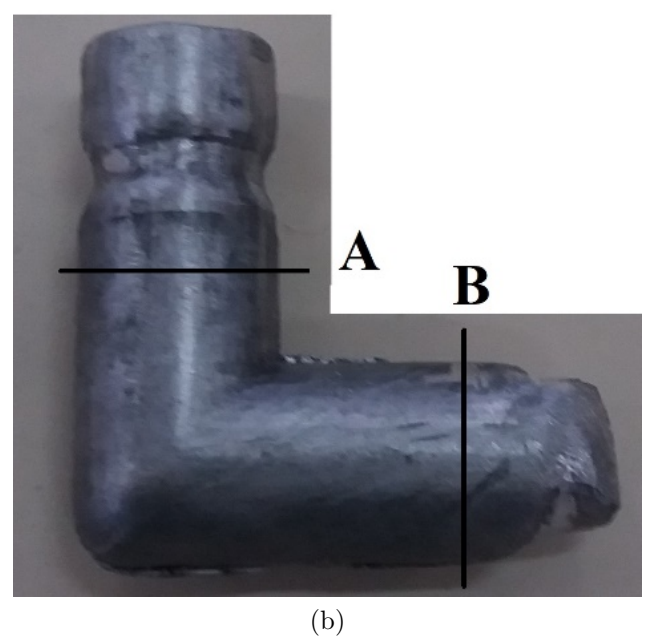


Fig. 10. a) Experimentally fabricated CP-Ti sample, and b) The position of the cross sections used for hardness measurements in the current designed CE-CAP die.

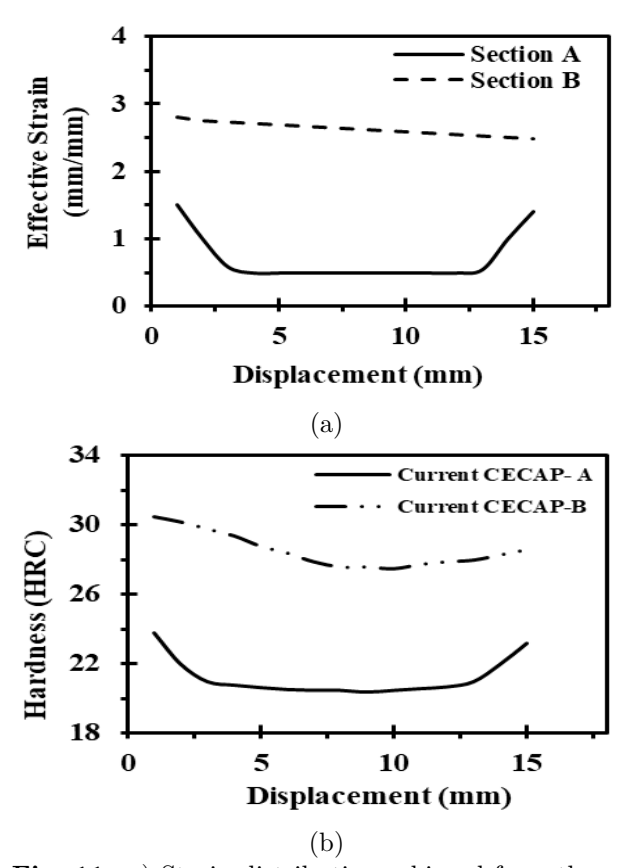


Fig. 11. a) Strain distribution achieved from the numerical study, and b) Hardness distribution obtained from experimental test on the cross section perpendicular to moving axis before and after ECAP zones shown by A and B, respectively, in the CECAP process.

7. Conclusions

Cyclic extrusion compression in equal channel angular pressing (CECAP) was studied to inspect the influence of the input variables including Temperature (T), input extrusion diameter (D), exit extrusion angle (α), frictional coefficient (μ) , and longitude distance of input extrusion to the ECAP region (L) on hydrostatic compressive stress (response parameter). Finite element analysis (FEA) and response surface method (RSM) were performed to carry out the study. The medical importance of CP-Ti has attracted the authors' attention to consider it as a case study. To quantify the hydrostatic compressive stress, the standard deviation (SD) was developed. RSM and analysis of variance (ANOVA) were employed to mathematically extract the model for the response and calculate the effectiveness of the parameters, respectively. Experimental tests and OM observation were carried out. Deform 3-D and Design Expert software were employed to numerically simulate the process and run the RSM experiments, respectively. Finally, the following conclusions can be drawn:

- Results revealed that factors A (temperature) and C (exit extrusion angle), and the interaction of AB (temperature and input extrusion diameter), AD (temperature and frictional coefficient), AE (temperature and longitude distance of input extrusion to the ECAP region), BE (input extrusion diameter and longitude distance of input extrusion to the ECAP region), and CD (exit extrusion angle and frictional coefficient) influence the hydrostatic compressive stress (σ) considerably.
- Moreover, the obtained outcomes showed that the frictional coefficient and longitude distance of input extrusion to the ECAP region are not significant factors in the current analysis.
- Comparison of the curvatures of surface plots shows that there is an interaction between temperature and input extrusion diameter which is in a good agreement with ANOVA results.
- Distribution of the hydrostatic compressive stress for four different processes on the cross section perpendicular to the moving axis was studied in the zones after first extrusion and before exit extrusion zones in the conventional CECAP (Input extrusion+ECAP), the new CECAP (Input extrusion+ECAP+Exit extrusion), and the current optimized CECAP respectively. The results showed an improvement for the current method compared to other approaches.

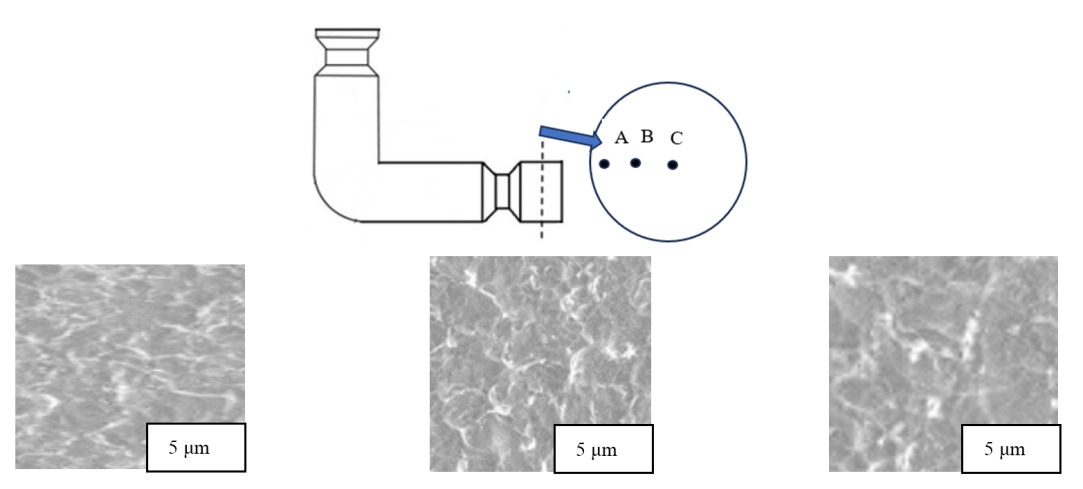


Fig. 12. OM observation for deformed CP-Ti extracted from transverse section (after exit extrusion zone) in the different positions.

- For lower ram speeds, the influence of the frictional condition on hydrostatic compressive stress for various angles shows an optimal point, meaning that the stress starts to fall after a certain value of the frictional condition.
- The results revealed that the increase of the ram speed causes the average of the stresses to be reduced slightly regardless of the frictional condition.
- At higher speeds, due to the lack of complete filling of the area between input extrusion and ECAP zones, and consequently reducing hydrostatic compressive stress, the values of the hydrostatic compressive stress start to drop for higher ram speeds.
- The outcomes show that as the exit extrusion angles rise, the hydrostatic compressive stress increases slightly in all domain of the horizontal axis (shown by exit extrusion angle).
- Hardness on the sections of fabricated specimens were measured and compared to the distribution behavior of the strain on the simulated specimens' sections. The results revealed that their variation trend is the same on the specimen section.
- The OM observation revealed that on the points to the outer surface of the CECAPed specimen, the grain size is more elongated.

References

[1] R. Valiev, Y.Estrin, Z. Horita, T. Langdon, M. Zehetbauer, Y. Zhu, Fundamentals of superior properties in bulk nanoSPD materials, Materials Research Letters, 4(2016) 1–21.

- [2] A. Azushima, R. Kopp, A. Korhonen, D. Yang, F. Micari, G. Lahoti, P. Groche, J. Yanagimoto, N. Tsuji, A. Rosochowski, Severe plastic deformation (SPD) processes for metals, CIRP Ann, 57(2008) 716–735.
- [3] M. Aghaei Khafri, N. Golarzi, Dynamic and metadyanamic recrystallization of hastelloy X superalloy, journal of materials science, 43 (2008) 3717-3724.
- [4] H.R. Rezaei Ashtiani, M. J. Ebrahimi, Investigate of microstructure evolution in hot extrusion for super alloy IN718, The tenth Conference of Manufacturing Engineering, anooshirvan university, babol, 2(2010) 34-44.
- [5] Y. Chehrehsaz, K. Hajizadeh, A. Hadjizadeh, L. Moradi, S. Mahshid, Effect of ECAP on Physicochemical and Biological Properties of TiO2 Nanotubes Anodized on Commercially Pure Titanium, Metals and Materials International, 4 (2021) 67-78.
- [6] K. Indira, U.K. Mudali, T. Nishimura, N. Rajendran, A Review on TiO₂ Nanotubes: Influence of Anodization Parameters, Formation Mechanism, Properties, Corrosion Behavior, and Biomedical Applications, J. Bio. Tribo. Corros, 3 (2015) 1-28.
- [7] S. Ahmadi, V. Alimirzaloo, G. Faraji, A. Donyavi, A New Modified Cyclic Extrusion Channel Angular Pressing (CECAP) Process for Producing Ultrafine-Grained Mg Alloy, Trans Indian Inst Met., 73(10) (2020) 2447–2456.
- [8] K. Hajizadeh, B. Eghbali, Effct of Two-Step Severe Plastic Deformation on the Microstructure and Mechanical Properties of Commercial Purity Titanium, Met. Mater. Int. 20, 343 (2014).

- [9] M. W. Richert Features of Cyclic Extrusion Compression: Method, Structure & Materials Properties, Solid State Phenomena, 114 (2006) 19-28.
- [10] N. Pardis, B. Talebanpour, R. Ebrahimi, S. Zomorodian, Mater. Sci. Eng. A 528, 7537 (2011).
- [11] S. Amani, G. Faraji, K. Abrinia, Microstructure and hardness inhomogeneity of fine grain AM60 magnesium alloy subjected to cyclic expansion extrusion (CEE), journal of manufacturing processes, 28 (2017) 197-208.
- [12] Langdon T.G., Superplasticity in ultrafine-grained materials, *Key Eng. Mater.*, 1994, 97(9): 109.
- [13] J. Zhang, K.-S. Zhang, W. Hwai-Chung, M.-H. Yu, Experimental and numerical investigation on pure aluminium by ECAP, Trans. Nonferr. Met. Soc. China 19(5) (2009) 1303-1311.
- [14] B.V. Patil, U. Chakkingal, T.P. Kumar, Influence of outer radius in equal channel angular pressing, World Academy of Science, Engineering and Technology. 62 (2010) 714-720.

- [15] M. Ensafi, G. Faraji, H. Abdolvand, Cyclic extrusion compression angular pressing (CECAP) as a novel sever plastic deformation method for producing bulk ultrafine grained metals, Materials Letters, 197 (2017) 12-16.
- [16] S. Ahmadi, G. Faraji, V. Alimirzaloo, A. Donyavi, Microstructure and Mechanical Properties of AM60 Magnesium Alloy Processed by a New Severe Plastic Deformation Technique, Metals and Materials International, 27 (2021) 2957–2967.
- [17] H. Ataeil, M. Shahbaz, H. S. Kim and N. Pardis, Numerical Analysis of Plastic Strain Inhomogeneity in Rectangular Vortex Extrusion (RVE) Process, Iranian Journal of Materials Forming 8(3) (2021) 46-52.
- [18] Y. Iwahashi, J. Wang, Z. Horita, M. Nemoto, T.G. Langdon, Principle of equal-channel anulgar pressing for the processing of ultra-fine grained materials, Scr. Mater. 35(2) (1996) 143–146.